

EBG Enhanced Dielectric Lens Antennas for the Imaging at Sub-mm Waves

J.J.A. Baselmans^{#1}, S. Yates^{#2}, A. Neto^{*3}, D. Bekers^{*4}, G. Gerini^{*5}, A. Baryshev^{#6}, Y.J.Y Lankwarden^{#7}, H. Hoevers^{#8}

[#] SRON Netherlands Institute for Space Research, Sorbonnelaan 2, 3584 CA Utrecht, The Netherlands

¹J.Baselmans@sron.nl

²S.Yates@sron.nl

⁶A.Baryshev@sron.rug.nl

⁷Y.J.Y.Lankwarden@SRON.nl

⁸H.F.C.Hoevers@sron.nl

^{*}TNO - Defence, Security and Safety, Oude Waalsdorperweg 63, 2597 AK, The Hague, The Netherlands

³andrea.neto@tno.nl

⁴dave.bekers@tno.nl

⁵giampiero.gerini@tno.nl

Abstract— We have designed a novel sub-mm radiation detector based upon a twin slot antenna placed in the focus of a Si elliptical lens. We use a novel Electromagnetic Band Gap (EBG) super-layer, consisting of $2 \frac{1}{4} \lambda$ dielectric layers of Si ($\epsilon=11.7$) and SiO₂ ($\epsilon=4$) and a Si carrier wafer to enhance the directivity of the feed. The antenna is coupled to a Kinetic Inductance Detector, KID, an extremely sensitive cryogenic radiation detector operating at 300 mK or lower temperatures. We present the design, implementation and measurements of the full detector, including optical sensitivity, frequency response and beam pattern.

I. INTRODUCTION

Truly integrated antennas in mm and sub-mm wave regimes can be realized by printing planar radiating elements in the focal plane of elliptical or extended hemispherical lens antennas [1], [2]. The elliptical shape of the lens gives high focusing properties provided that its eccentricity is properly related to its dielectric constant ($e=1/\sqrt{\epsilon_r}$). In the frame of cooperation activity between TNO and SRON, the main purpose of this contribution is to present a new way to increase the directivity of the focal plane feeds typically used to excite such lenses. The driving reason for this effort is the desire to diminish the impact of the reflections at the dielectric air interface when these structures are proposed as focal plane imagers.

The number of elements that can be located in the focal plane of a dielectric lens is limited because the performances of the elements located at a large distance from the central focus are significantly degraded with respect to the elements in focus [3]. This effect can be interpreted as low spill-over efficiency of the lens since a significant portion of the power radiated by the feeds is intercepted by the dielectric-to-air interface at locations that do not directly contribute to a focused beam. To increase the number of radiators on the ground plane, elements of larger directivity should be used so that they all excite efficiently the central portion of the lens is

larger. This solution is effectively equivalent to increasing the F/D of the lens system.

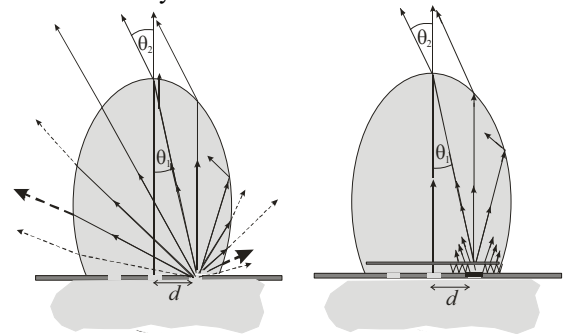


Fig. 1 Ray picture in the case of an off focus fed dielectric lens, with and without leaky wave enhancement by means of EBG super-layer.

II. EBG ENHANCED DIELECTRIC LENSES

Recent investigations indicate that Electromagnetic Band Gap (EBG) super-layers can be used to enhance the directivity of planar and waveguide antennas. In particular, in [4] and [5], the efficient excitation of reflector antennas by means of EBG enhanced printed waveguide feeds has been discussed in depth. The main result is that the efficiency of single-feed reflectors and imaging arrays can be increased significantly with respect to radiators operating in free space, at low to moderate manufacturing cost. Here a similar design strategy has been applied to increase the efficiency of dielectric lens antennas. While the use of EBG super-layers at microwave frequencies was justified mainly by the electric performances of the systems, the manufacturing advantages of the EBG solutions based on dielectric may end up being the most important criteria in the sub-mm wave regimes. This particular difference can be understood from the intrinsic difficulty in realizing corrugated waveguide horns with micrometric

accuracies and the integration of these horns with the receivers could be insurmountable.

III. INVERTED DIELECTRIC STRATIFICATION.

The guidelines for a dielectric stratification to realize the optimal Fabry-Perot resonator, also referred to as EBG structure, have been clarified to the antenna community by Jackson and Oliner in [6], who provided a leaky-wave interpretation of the phenomenon. Two dominant (TE/TM) leaky waves are sufficient to represent main radiation in directions close to broadside. If the upper layer is a dielectric lens antenna (Fig. 2) instead of free space a series of quarter wavelength transformers will create an equivalent input impedance z_{in} that is very large instead of very small. In this way, a virtual open circuit or magnetic conductor is created. As depicted in Fig. 2, layer (0) is then a quarter of the dielectric wavelength, shorted by a ground plane at $z=0$. Consequently, the field configuration of a waveguide with a lower electric wall and an upper magnetic wall is created. At every bounce in the positive z direction there is some power leaked in higher stratifications which eventually leads to radiation in the dielectric.

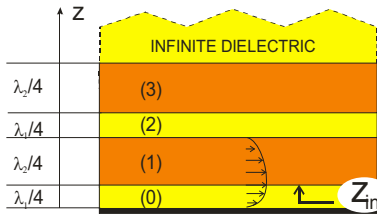


Fig.2 Dielectric stratification to achieve directivity enhancement for a structure radiating in an infinite dielectric.

IV. DESIGN OF THE PRINTED RADIATORS

The wave picture just described can be rigorously represented by identifying the two dominant poles in the Green's Function of the dielectric stratification. The directivity enhancement that can be achieved depends on the equivalent impedance contrast which is observed at z_{in} . Given a fixed ratio between ϵ_{r1} and ϵ_{r2} such contrast can be enhanced to achieve higher directivities by using a larger number of dielectric super-layers. However, such an increase of contrast leads to a smaller operating BW.

The trade-off between the BW and the directivity guides our design, in which only one layer of dielectric constant $\epsilon_{r1} = 4$ (quartz) is applied to enhance the radiation in the lens of $\epsilon_{r2} = 11.7$ (silicon). For our design, we decided to initially choose 10 GHz as design frequency, for which we had already acquired experience in [5]. Accordingly the lower slabs are 2.4 mm for the silicon layer and 3.75 mm for the quartz layer. A double slot radiator is designed, see Fig. 3a. The central radius $(R_{in}+R_{out})/2$ of this slot is set in such a way that an optimal excitation of the lens is achieved by minimizing the influence of higher order modes as in [4]. The width of the slots affects their impedance bandwidth while the length of

each arc (defined by the angle θ) sets the central operating frequency. A nominal design with slabs tuned to 10 GHz operates well on a 10% BW centered around 10.5 GHz for the following parameter choices: $R_{in}=2.6$ mm, $R_{out}=3.2$ mm, $a=22^\circ$. The radiation pattern of the double-slot structure calculated at 10.5 GHz with the commercial software CST (FDTD) is presented in Fig. 3b. One can observe the almost perfect symmetry of the pattern as a function of the azimuth angle as well as the rapid drop-off, which starts at about 30° . These properties ensure that the silicon dielectric lens excited by the twin slot will have a high spill-over efficiency.

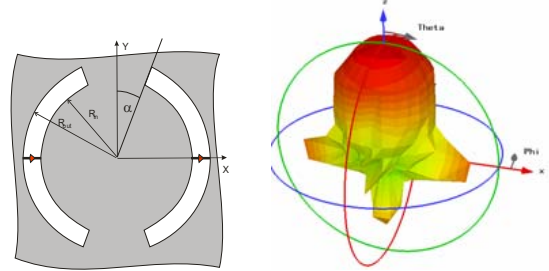


Fig. 3 Double slot configuration a) to achieve symmetric patterns b) and cancellation of higher order modes

V. SUB-MM WAVE IMPLEMENTATION

After the preliminary design at 10.5 GHz, a prototype of an antenna system was manufactured for operation at $F_{RF}=675$ GHz. This prototype consists of the (scaled) antenna as shown in Fig.3, with $R_{in}=40.4$ μm , $R_{out}=49.8$ μm , $a=22^\circ$, integrated with a Kinetic Inductance Detector (KID), as currently developed by SRON (7,8). We need to mention here that, for the time being, KIDs are realized with a technology based on the use of a dielectric slab that hosts a metallic printed structure. Since such a structure will have to host both the slot antennas and the feeding structure, the only available solution is to use coplanar waveguide (CPW) feeding lines. Each of the two slots is therefore excited with a CPW line and the two lines are connected in parallel to achieve a unique feed. A picture of the KID-antenna detector is given in Fig. 4. The devices are made of a 150 nm sputter deposited Ta film with a 6 nm Nb seed layer to promote the growth of α -Ta (9). As substrate we used either a plain Si wafer or a custom made tri-layer wafer with one $\frac{1}{4} \lambda$ section of Si (36.2 μm) and one $\frac{1}{4} \lambda$ section SiO_2 (59.2 μm) and a thick (436 μm) Si capping layer. A 3.6 mm diameter elliptical lens is glued to the capping layer of the chip with the antenna feed in the second focus.

To be able to measure the beam pattern and frequency response of the antenna we mount the device on a He3 cooler, with a base temperature of 300 mK, inside a He4 cryostat. The lens is aligned to the antenna and attached to the chip backside using super glue. The lens-chip combination is mounted in a special sample holder with the lens in front of the cryostat window. Wire bonds connect the chip ground plane to the box walls and also connect each end of the central line of the through line (referring to Fig.4) to a TMM circuit board. The latter are connected to standard SMA panel launchers. 2 coaxial cables run from the sample holder to the cryostat

exterior. To be able to measure the optical sensitivity we use the same sample holder but mount it in an Adiabatic Demagnetization Cooler, with a base temperature of 30 mK, which is equipped with a cryogenic (3-20K) black body radiator as calibration load.

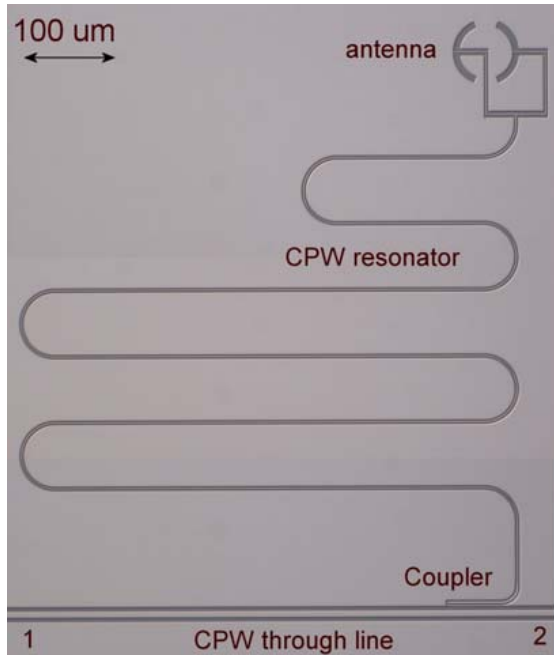


Fig. 4: Micrograph of a KID with a 675 GHz antenna. Contacts 1 and 2 of the through line are connected to two coaxial cables. The length of the CPW resonator sets the resonance frequency, the geometry of the coupled sets the resonator Q factor.

The device works as follows: In a superconducting material at temperatures $T \ll T_c$, the critical temperature, all conduction electrons are condensed into a single quantum-mechanical ground state of paired electrons, Cooper pairs. These paired particles do not contribute to electric losses but have a non-negligible (kinetic) inductance. Referring now to Fig. 4 we see that the antenna is an integral part of the KID resonator. Radiation absorbed by the antenna is direct into the CPW feeds towards a summing point where it enters the main CPW line of the KID resonator. Since the F_{RF} (675 GHz) is larger than the gap frequency of Ta (340 GHz) the RF radiation breaks superconducting Cooper pairs into quasiparticle excitations. As a consequence the RF radiation decays over several wavelengths ($\lambda=250 \mu\text{m}$) in the KID CPW. The KID resonator is able to detect these quasiparticles as follows: The CPW resonator (Fig. 4) is a $1/4\lambda$ CPW resonator, capacitively coupled to another CPW line, the through line, and shorted at its far end at the antenna feeds. The resonator length $L_{\text{resonator}}=c'/4F$, with $c'=c/\sqrt{\epsilon_{\text{eff}}}$ and c the speed of light, which corresponds to a resonance frequency $F' \sim 4 \text{ GHz}$ for a 5 mm long resonator. The Q factor of the resonator can be changed between 10^3 and 10^6 by changing the coupler geometry (7,8). The inductance of the resonator is given by its geometrical and kinetic inductance, the latter being proportional to the Cooper pair number. Breaking Cooper pairs changes thus the total inductance of the

resonator, shifting the resonance frequency to lower values. By sending a readout signal identical to the resonance frequency in equilibrium through the through line (1-2 in Fig.4) any signal at the antenna breaks Cooper pairs, which are detected by a change in the phase transmitted at resonance. It has to be noted that $F_{RF} \gg F'$, so the presence of the antenna only slightly modifies the resonator properties when compared to a similar CPW resonator without antenna.

The main purpose of this integration is to demonstrate the effectiveness of the detector in combination with a leaky-wave enhanced antenna. At the time of writing we have started with the initial measurements, the results of which will be presented at the conference and in the final version of this manuscript.

REFERENCES

- [1] D.F. Filippovic, S.S. Gearhart, and G. M. Rebeiz: "Double Slot on Extended Hemispherical and Elliptical Silicon Dielectric Lenses" *IEEE Trans. Microwave Theory Tech.*, 1993, Vol. 41, Issue 10.
- [2] P. Focardi, R. Mc Grath, A. Neto "Design Guidelines for THz mixers and Detectors", *IEEE Trans. on MTT*, Vol. 53, no. 5 May 2005
- [3] Wu, X.; Eleftheriades, G.V.; van Deventer-Perkins, T.E.; Design and characterization of single- and multiple-beam mm-wave circularly polarized substrate lens antennas for wireless communications *Microwave Theory and Techniques, IEEE Transactions on* Vol. 49, No. 3, March 2001 Page(s):431-441
- [4] Nuria Llombart, Andrea Neto, Giampiero Gerini, Magnus Bonnedal, Peter De Maagt, "Leaky Wave Enhanced Feed Arrays for the Improvement of the Edge of Coverage Gain in Multi Beam Reflector Arrays", accepted for publication on *IEEE Transactions on Antennas and Propagation*,
- [5] A. Neto, N. Llombart, G. Gerini, M. Bonnedal, P. de Maagt, "EBG Enhanced Feeds for High Aperture Efficiency Reflector Antennas", on the *IEEE Transactions of Antennas and Propagation*, Vol. 55, no.7, August 2007
- [6] D. R. Jackson, A. A. Oliner, "A leaky-wave analysis of the high-gain printed antenna configuration", *IEEE Transactions on Antennas and Propagation*, Vol. 36, no. 7, pp. 905-909, July 1988.
- [7] P. Day, H. leDuc, B. Mazin, A. Vayonakis, J. Zmuidzinas, "A broadband superconducting detector suitable for use in large arrays", *Nature* **425**, 817-820, (2003).
- [8] J.J.A. Baselmans, S.C.J. Yates, R. Barends, Y.J.Y. Lankwarden, J.R. Gao, T.M. Klapwijk, "Noise and sensitivity of aluminum kinetic inductance detectors for sub-mm astronomy". Presented at the 12th international Low Temperature Detectors conference, July 22-27, Paris (2007).
<http://springerlink.metapress.com/content/958t38200823qj3t/fulltext.pdf>
- [9] D. W. Face and D. E. Prober, *J. Vac. Sci. Tech. A* **5**, 3408 (1987).